Bulletin of Pure and Applied Sciences. *Print version ISSN 0970 4639*
Vol.38 F (Geology), No.2, *Online version ISSN 2320 3234*
July-December 2019: P.246-265 *DOI: 10.5958/2320-3234.2019.00019.2*

Available online at www.bpasjournals.com

Original Article

Evaluation of Groundwater Potential and Aquifer Protective Capacity of the Overburden Units in Trap Covered Dhule District, Maharashtra

Khan Tahama[1], Gautam Gupta[1,], M.V. Baride[2], J.B. Patil[2] and Arti Baride[2]*

Author's Affiliations:
[1]Indian Institute of Geomagnetism, New Panvel (W), Navi Mumbai 410218, India.
[2]Department of Geology, Z.B. Patil College of Arts, Science and Commerce, Dhule 424002, India.

***Corresponding Author: Gautam Gupta**, Indian Institute of Geomagnetism, New Panvel (W), Navi Mumbai 410218, India.

E-mail: gupta_gautam1966@yahoo.co.in

(Received on 04.10.2019, **Accepted on 04.11.2019**)

ABSTRACT

This paper illustrates the determination of overburden protective capacity using vertical electrical resistivity sounding in the semi-arid hard rock terrain in Dhule district of Maharashtra. A total of 54 vertical electrical soundings (VES) were carried out using Schlumberger configuration with maximum electrode separation of 200m. The objective of this study was to locate groundwater potential zones and to evaluate the protective capacity of aquifers. Results reveal that the longitudinal conductance (S) value ranges from 0.07 to 13 mhos (siemens). The overburden protective capacity of the aquifers reveals a good to moderate rating at 92% of the VES sites. While 2% each represent weak and poor rating, 4% fall in the excellent category. It is further observed that VES sites located towards north at Sirpur and northern Sindkheda sub-divisions have better protection to aquifers due to thick alluvial cover deposited by Tapi River. The transverse resistance reveals higher values towards north-west, east and south-east parts of the study area. Electrical anisotropy shows a large variation ranging from 1.028 to 6.55, implying heterogeneous and anisotropic nature of the subsurface in the study area. A positive correlation is observed between the fracture porosity and electrical anisotropy, indicating the porous zones in the study area. Further, stations with low reflection coefficient revealed higher electrical anisotropy, suggesting an inverse correlation between these two parameters. These results provide reliable information about the protective capacity of the geomaterials overlying the aquiferous unit and the fracture geometry using various geophysical indices. This is vital for planning and development of prospective water resource programs and serves as a guide for groundwater pollution control in hard-rock, semi-arid regions.

KEYWORDS: *Protective capacity, electrical anisotropy, fracture porosity, reflection coefficient, Dhule*

1. INTRODUCTION

The impact of urbanization and industrial development has put a negative stress on the biosphere. The rate at which the development is taking has an adverse bearing on water resources more than any other natural resources in particular, as water is considered an important natural resource.

There is relentless water paucity in Deccan Volcanic Province (DVP) of Maharashtra and there is urgency in locating secondary sources of groundwater almost all over the region. Being a hard rock terrain, it is all the more challenging to delineate potential groundwater pockets. It is reported that these groundwater zones are located in the weathered and fractured part of the Deccan Traps (Rai et al., 2013). Deolankar (1980) is of the opinion that groundwater in such trap covered area is due to secondary porosity and permeability resulting from weathering and fracturing.

Amongst all geophysical techniques, the electrical resistivity method has been extensively employed for delineating the sub-surface layers in order to understand the hydrogeological set-up of a region (Zohdy et al., 1974). Several researchers have worked towards the hydrogeological aspects in this trap-covered country. Geophysical studies carried out by Rai et al. (2013) demarcated aquifers in intertrappeans/vesicular and fractured zones within and below the trap sequence. The Dhule district is infested with dykes and therefore bears a significance in hydrogeological set up in the hard rock terrain like DVP (Singh and Jamal, 2002; Duraiswami, 2005). Several workers have classified the dykes as carrier or barrier to the groundwater flow depending upon strength of fracturing in them (Singh and Jamal, 2002; Nilsen et al., 2003). It is thus pertinent to delineate the groundwater resources in such hard-rock environment.

Attempts have been made in Panjhara watershed, Dhule district, to delineate the carrier and barrier stretches within the dykes and the depth to which these dykes holds potential to accumulate groundwater and subsequent transmission using vertical electrical resistivity sounding (VES) and ground magnetic survey (Erram et al., 2010). These studies indicated that dykes form potential and distinct aquifers in the area, as they have sufficient width, length and favorable hydrogeological structure. It is also revealed that dykes behave as a medium for groundwater flow, provided porosity and permeability characteristics of dyke rocks are superior to the host rock and their trends in relation to topography are pertinent (Erram et al., 2010). In a recent study, Baride et al. (2017) used resistivity technique to study the subsurface lithology of Dhule region with an aim to differentiate the aquifers and delineate the depth of aquifers and comparison between Wenner and Schlumberger methods.

Being a water-scarce region, it is of utmost requirement to recommend the development plan for groundwater and surface water management. It is also indispensable to comprehend the exploration and exploitation for groundwater. In this work, vertical electrical resistivity sounding data has been analyzed in order to examine the sub-surface features in Dhule district, Maharashtra. The objective of this study is to perceive the lateral and vertical limits of the aquifers, to assess the Dar-Zarrouk indices and to estimate the aquifer protective capacity ratings in the study area, so as to provide a constructive solution in delineating the fresh water aquifers in the trap covered area. These parameters will also reveal the anisotropic characteristics of fractures which are vital for sustainable groundwater development (Shailaja et al., 2016).

2. STUDY AREA

Dhule district covers an area of 8063 sq. km. which is about 2.6% of the total land of the state of Maharashtra (Fig. 1). It is included in the Survey of India Toposheet Nos. 46 G/16, H/13, K/4, K/7, K/8, K/11, K/12, K/14, K/15, K/16, L/1, L/4, L/5, L/9, L/10, L/13, L/14, O/2, O/3, O/4 (CGWB, 2013). This district consists of four sub-divisions viz. Dhule, Shirpur, Sindkheda and Sakri. The major occupation of this area is agricultural activities and depends on groundwater for irrigation.

The Dhule district is covered in Upper Tapi basin which forms the northern most part of Maharashtra state. It is bounded by 20º 38″ to 21º 60″ North latitude and 73º 50″ to 75º 11″ East longitudes. Dhule district is bounded by Jalgaon district in the east, Nasik district forms the southern end, on the northern part is the Nemad district in Madhya Pradesh, and Nandurbar district is in the western side.

Several major rivers like Tapi, Panjhara, Burai, Arunavati, Aner, Bori, Kan and Amravati traverses the Dhule district. The Panjhara River is the longest (about 136 km) and drains through Sakri, Dhule and Sindhkheda sub-divisions. The Tapi River flows through Shirpur and Sindkheda sub-divisions and enters Nandurbar district into Ukai dam in Gujarat state. These rivers are the major source for surface and groundwater in the district.

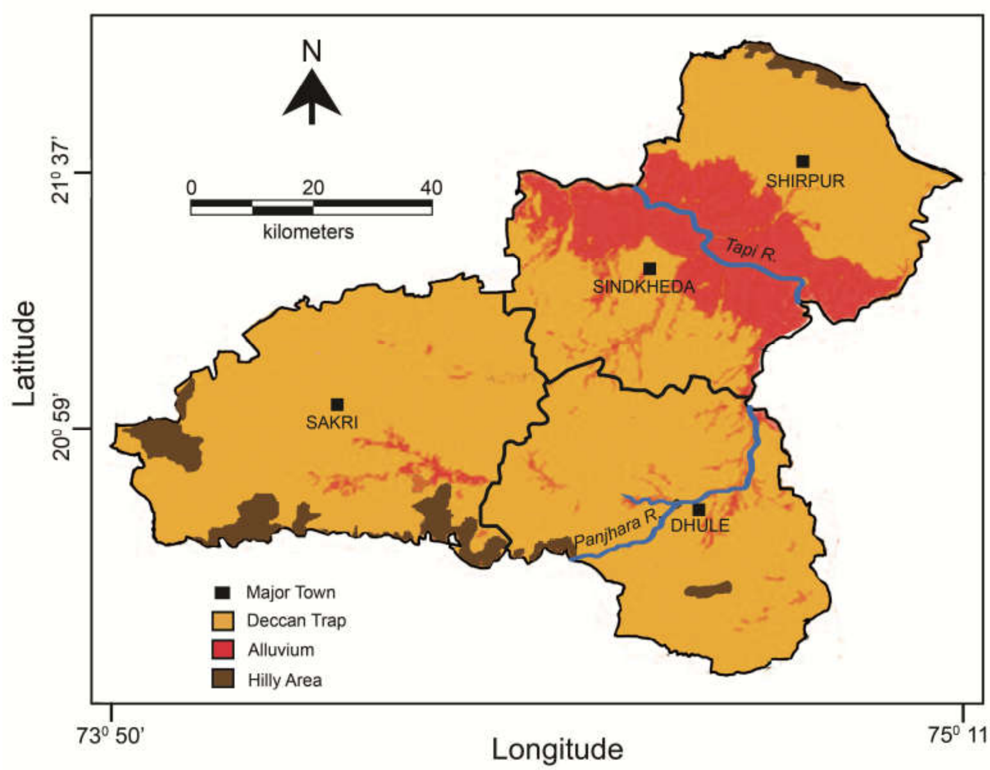

Figure 1: General geological map of Dhule district.

The soils of the district are derived from basalt and from the river system. Alluvium is dominant along the rivers and along hill slope streams, south of Tapi valley, which is light soils, dark brown to yellowish brown, loamy to clay loamy texture with sub angular grains. The medium soil is supposed to be good for irrigation and is found between Tapi and Panjhara river valley in Sindkheda, Sakri and southern part of Dhule sub-divisions, whereas low, medium and black cotton soil is found in Shirpur and Sindkheda sub-divisions.

Dhule district is hot and dry, arid to semi- arid type climatic conditions. The mean maximum and minimum temperature is 45°C and 16°C respectively. Higher relative humidity of the order of 75% with high temperature is expected in the months of May and October. This district receives monsoon during July, August and September and the annual average rainfall ranges from 499 to 864 mm. It is reported by CGWB (2013) that minimum rainfall occurs in the central parts of the district around Dhule, Sakri and parts of Sindkheda, while it increases northwards towards Shirpur and westwards.

Rainfall is the main factor that determines cropping pattern and agricultural operations. Major part of the district falls under scarcity zone, with Dhule, Sindhkheda and eastern part of Sakri being the most affected. Some parts of Shirpur sub-division falls in the assured rainfall zone (CGWB, 2013). The major agriculture produce in this region is bajara, jowar, wheat and cash crops like cereals, cotton, groundnuts, banana and sugarcane are also produced.

3. GEOLOGY AND HYDROGEOLOGY

Deccan Volcanic Province (DVP) is the largest igneous province of India and best exposed continental flood basalt of the world (Sheth, 2005; Subbarao et al., 1988). The crust in DVP is covered by the fissure erupted basaltic magma, spreading over an area of about half a million sq. km. in the western part of the Indian peninsula. The continental flood basalts with thickness ranging from a few meters to about 2000 meters are emplaced over the northern part of the Dharwar craton (Qureshy, 1981), which has suffered severe tectonic activity during the Precambrian. Furthermore, the isostatic imbalance caused by the nearly 10^{15} tons of the basalts as well as the subsequent weathering and erosional processes may have made a significant contribution to the tectonic evolution of the DVP (Widdowson and Mitchell, 1999).

The Deccan volcanism was active at the Cretaceous-Tertiary boundary and at present up to about 29 basaltic lava flows has been documented in different parts of the Deccan volcanics (Wadia, 1975). The Deccan trap is divided into three sub-groups (Kalsubai, Lonavala and Wai) which consist of twelve different formations. The Kalusbai sub-group forms the base consisting of five lower formations starting from the bottom Jawhar, Igatpuri, Neral, Thakurwadi and Bhimashankar formations (Beane, et al., 1986, Subbarao et al., 1994). These are separated by Kashele Giant Plagioclase Basalt (GPB) flow, typically presetting mega-porphyritic texture with phenocrysts of plagioclase, ranging in length from few mm to over a centimeter (GSI, 2001). The topmost part of the Mg-rich olivine phyric basalts of Igatpuri formation is exposed along Panjhara river bed (Beane, et al., 1986; Subbarao et al., 1994).

The primary openings in the basaltic flows are inadequate and thus have low porosity and permeability for occurrence of groundwater. Though cavities, vesicles, etc. in the basaltic rocks of Dhule district (Fig. 1) can increase the porosity (Pawar and Shaikh, 1995), but the flows here are relatively nonporous rocks. However, jointing and fracturing of these rocks give rise to secondary porosity and permeability ideal for incidence of groundwater.

The vesicular crust is the main water-bearing horizon in compound flows of Thakurwadi formation in the study area. These flows are perhaps weathered at the surface down to the depth of about 10-15 meters depending upon local slope. Beneath the weathered zone, the rocks portray variable degree of fracturing and jointing that reduce with depth. Therefore, only the shallow water table aquifers are broadly developed in the area.

Numerous doleritic dykes cut across the basaltic lava flows from the study area. The dyke features are copious in southern part, while only three dykes are reported in northern part of the study area. The E-W trending dykes are prevailing and follow Narmada-Son regional tectonic trend (Deshmukh and Sehgal, 1988). These are older than the NW-SE trending dykes that reflect younger phase of intrusion (Deshmukh and Sehgal, 1988). Geophysical investigations revealed that dykes form potential and distinct aquifers in the area, as they have sufficient width, length and favorable hydrogeological structure. Also dykes behave as a medium for groundwater flow provided porosity and permeability characteristics of dyke rocks are superior to the host rock and their trends in relation to topography are pertinent (Erram et al., 2010).

The groundwater occurs in the near surface strata down to the depth of 20 m under unconfined conditions in the weathered zone, vesicular/amygdaloidal basalt, jointed and fractured massive basalt. The water bearing strata occurring below 30 m depth, beneath the red bole and dense massive basalt, exhibit semi-confined to confined conditions. In the foot hills zone the water table is relatively shallow and in the valleys and plains of river basin, the water table aquifer occurs at shallow depth and the wells in such areas do not go dry and sustain perennial yield except in extreme summer or drought conditions. The yield of the dug wells varies from 60 to 125 m^3/day, whereas those of bore wells varies from 2 to > 20 m^3/hr, however in most of the bore wells it ranges between 2 to 10 m^3/hr (CGWB, 2013).

The alluvium strata are encountered down to depths of 100 m at certain places in the north of the study area. Groundwater occurs under water table in semi-confined and confined conditions in inter granular pore spaces of gravel and sand. The yield of the dug wells varies between 150 and 200 m^3/day, whereas that of exploratory wells varies from 1.50 to 6.00 lps. The yields of the tube wells drilled ranges from 20 to 250 m^3/hr (CGWB, 2013).

4. MATERIAL AND METHODS

The resistivity survey is based on measuring the potentials between one electrode pair while transmitting the current between another electrode pair. The depth of penetration is directly proportional to the separation between the electrodes in homogeneous ground, and varying the electrodes separation provides electrical information about the foliation of the ground (Dahlin, 2000). For the present study, a total of 54 Vertical Electrical Soundings (VES) were acquired (Fig. 2) using Schlumberger configuration with maximum electrode spacing (AB) of 200 m. The instrument used is Resistivity meter MINITRONIX model AQUA II and AQUA II PLUS. The obtained apparent resistivity data is processed and interpreted using IPI2Win software (Bobachev, 2003). The apparent resistivity (ρ_a) vs. half of the current electrode separation (AB/2) on double-log graph suggests 4-6 layered structure in the study area (Table 1a). This procedure helps to obtain the first order geoelectric parameters viz. true resistivity (ρ) and true thickness (h) values for each sub-surface layers, which leads to the computation of the second-order geoelectric parameters, the longitudinal conductance (S) and transverse resistance (T), also known as Dar-Zarrouk (DZ) parameters termed after Maillet (1947). These parameters help to overcome the ambiguities in interpretation due to suppression and equivalence of layers and may be of great help to study the hydrological properties of the aquifers (Henriet, 1976). Also the overburden aquifer protective capacity is estimated from longitudinal conductance (S), which in turn reveals about the percolation of contaminants if any. Apart from S and T, other geoelectric indices, i.e. transverse resistivity (ρ_t), longitudinal resistivity (ρ_l) and electrical anisotropy (λ) for every VES station has been computed after Zohdy et al. (1974) (Table 1b).

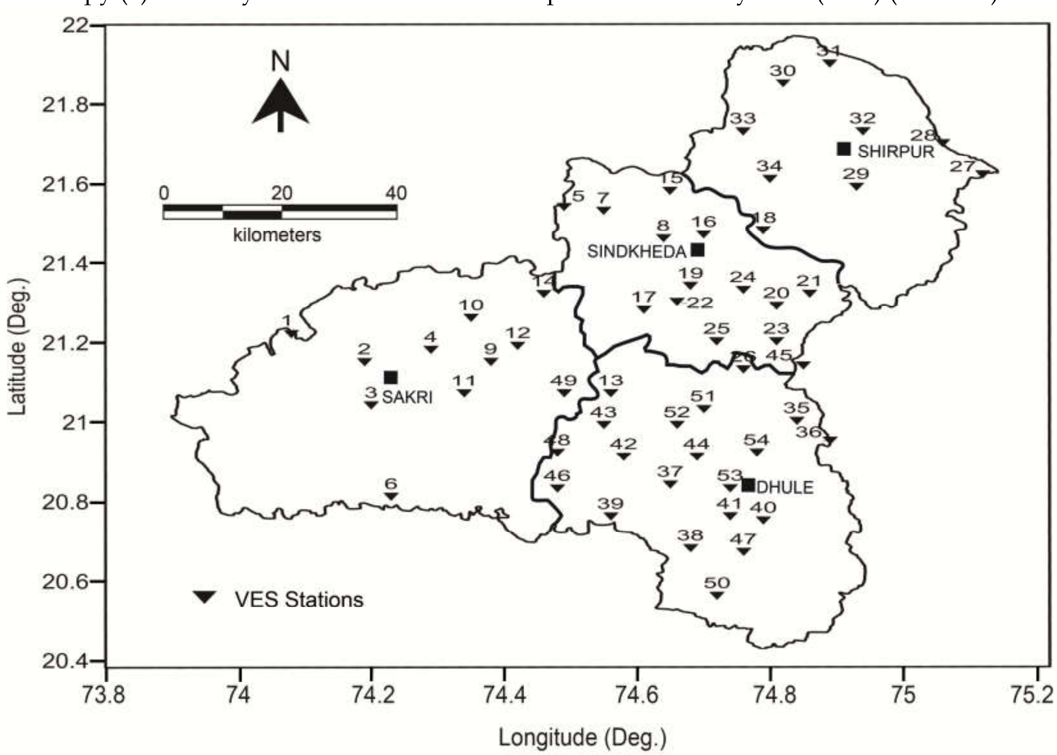

Figure 2: Location map of the study area showing the VES surveying points

Table 1(a): Summary of VES data interpretation and qualitative analysis of curve types in Dhule district

	Layer resistivity (Ωm)						Layer thickness (m)					
VES NO.	ρ_1	ρ_2	ρ_3	ρ_4	ρ_5	ρ_6	h_1	h_2	h_3	h_4	h_5	Curve type
1	52.3	8.43	134	24	111	16.2	0.68	0.258	0.49	1.09	88.9	HKH
2	40.8	3.87	65.7	901	9.5	243	0.5	0.0717	9.3	3.37	1.55	HAK
3	61.6	107	1048	86.3	10401	---	0.935	2.16	4.57	45.2	---	AKH
4	29.7	28.5	3027	1.73	148	3.62	0.849	0.987	0.0698	0.307	97.4	HKH
5	25.5	220	18	196	413	1530	0.5	0.425	0.577	16.3	82.2	KHA
6	35.9	8.44	188	36.4	134	387	0.545	0.118	0.307	0.778	15.7	HKH
7	36.4	46.2	378	87	1458	95.8	0.5	3.79	0.0748	16.2	6.03	AKH
8	5.46	29.6	213	48.6	153	130	0.5	0.836	2.23	5.96	15.9	AKH
9	114	45.9	11.8	36.3	368	35.4	0.5	1.61	0.529	16.8	8.12	QHA
10	46.2	22.7	228	0.498	---	---	1.33	11	11.1	---	---	HK
11	43.2	26.2	69.9	28.7	8.66	222	0.553	0.624	0.707	8.6	7.45	HKQ
12	42.8	127	50.2	106	229	16.5	1.56	0.21	6.15	31.5	42.1	KHA
13	4.23	665	18.8	2627	21.3	1307	0.5	0.385	2.34	3.19	10.3	KHK
14	32.5	22.4	10.9	528	52.2	3155	0.5	2.33	2.09	0.571	55.4	QHK
15	38.5	11.9	69.2	270	23.5	184	0.516	0.246	7.66	5.27	5.14	HAK
16	52.8	4.05	134	725	13	101	0.968	0.639	0.399	2.54	2.29	HAK
17	28.7	30	28	30.9	148	46.6	0.882	2.25	2.54	29.5	22.3	KHA
18	23.7	3.53	76.3	10.5	71.4	5995	0.513	0.455	0.198	9.62	53	HKH
19	51.1	214	27.7	565	194	11	0.96	0.848	1.38	1.2	78.6	KHK
20	38.4	5.09	29.6	724	35.8	8.14	0.618	0.109	8.16	24	35.1	HAK
21	51.1	214	27.7	565	194	11	0.96	0.848	1.38	1.2	78.6	KHK
22	16.3	46.7	426	600	11.9	1.82	0.5	2.03	28	11.8	15	AAK
23	17.9	151	12	114	997	2.62	0.6	0.652	0.409	18.6	18.3	KHA
24	14	477	8.56	218	7186	26.4	0.5	0.252	0.978	19.3	3.01	KHA
25	23.2	56.8	15.7	66.6	11156	9.55	1.25	8.427	4.05	11.3	1.22	KHA
26	18.4	10.3	32.6	86.9	412	3.17	0.501	0.14	2.08	23.9	12.1	HAA
27	2.9	172	0.347	8.47	133	1.1	0.5	0.396	0.0799	22.1	11.7	KQH
28	22.9	9.91	1.92	6.79	266	2.03	0.5	2.8	0.633	21.6	8.23	QHA
29	8.76	196	3.17	1077	11317	44.1	0.5	0.326	1.62	7.09	72.5	KHA
30	20.5	231	4.82	165	5481	10.6	0.5	0.508	2.46	1.45	5.08	KHA

	Layer resistivity (Ωm)						Layer thickness (m)					
VES NO.	ρ_1	ρ_2	ρ_3	ρ_4	ρ_5	ρ_6	h_1	h_2	h_3	h_4	h_5	Curve type
31	3.27	57.1	2.2	287	6648	249	0.503	0.678	2.19	4.62	74	KHA
32	23.1	9.43	1.74	6.85	281	2.03	0.5	2.98	0.618	20.9	7.42	QHA
33	4.83	71.9	2.09	180	7217	11.4	0.571	0.564	1.95	1.11	3.22	KHA
34	19.8	114	20.2	3.02	17.6	---	0.953	0.277	9.98	2.36	---	KQH
35	19.8	12.5	155	25.5	162	6.56	0.738	0.496	1.1	3.48	72	HKH
36	18.1	1.15	352	5.24	68230	18.1	0.54	0.156	0.659	4.53	0.441	HKH
37	118	9.57	134	150	2572	2.99	0.521	0.157	6.36	0.402	7.8	HAA
38	144	108	2167	323	224	6.28	0.507	0.536	0.169	26.6	41	HKQ
39	64.1	2.98	1031	16.8	2143	200	0.5	0.106	0.34	3.05	2.51	HKH
40	27.5	522	28.7	181	932	---	0.645	0.848	0.407	98.1	---	KHA
41	35	3.62	124	248	41.7	2927	0.5	0.0686	14.3	9.84	22.3	HAK
42	5.86	19.6	10.4	1424	5.09	0.957	1.81	0.164	0.607	4.93	17.9	KHK
43	116	138	578	80.9	190	302	0.508	3.38	4.5	11.8	17	AKH
44	173	706	79	2040	8.54	723	2.02	0.944	2.08	9.61	6.93	KHK
45	3.97	1165	16.2	107	0.356	723	0.729	0.0267	7.66	21.7	4.33	KHK
46	12.4	78.1	16.2	63.4	2.79	723	0.729	0.0266	1.73	29.6	1.66	KHK
47	355	115	390	27.5	497	0.916	0.517	7.34	3.01	7.38	12.2	HKH
48	5.55	67.3	5.6	34	1103	0.916	1.08	0.7448	2.49	7.88	4.08	KHA
49	15.5	0.755	5701	1455	5.55	0.916	0.5	0.249	0.368	3.25	61.9	HKQ
50	299	3.84	3719	42.9	190	0.916	0.706	0.19	0.177	3.3	95.6	HKH
51	243	1.87	6606	23.8	484	0.916	0.5	0.138	0.102	3.16	42.4	HKH
52	6.47	3.29	184	675	145	19.7	0.875	0.0635	3.94	0.392	94.7	HAK
53	7.5	0.582	29.1	151	177	19.7	0.875	0.0448	3.96	0.392	94.7	HAA
54	12.3	451	16.2	4859	88.8	12	0.875	0.0296	3.71	0.198	92.9	KHK

Table 1(b): The computed Geoelectric (Dar-Zarrouk) Parameters for Dhule district

VES NO.	H (m)	T (Ωm^2)	S (Seimens)	ρ_t (Ωm)	ρ_l (Ωm)	λ	ϕ_f	*Aquifer Protective capacity	Reflection Coeff.
1	91.42	9997.46	0.894	109.36	102.31	1.03	0.001	G	-0.745
2	14.79	3682.78	0.339	248.97	43.60	2.38	0.071	M	0.925
3	52.87	8978.83	0.563	169.84	93.82	1.34	0.001	M	0.984
4	99.61	14680.36	0.899	147.37	110.83	1.15	0.001	G	-0.952
5	100.00	37260.04	0.336	372.59	297.81	1.11	0.001	M	0.575
6	17.45	2210.39	0.169	126.68	103.04	1.1	0.003	W	0.486
7	26.59	10422.71	0.286	391.90	92.89	2.05	0.032	M	-0.877
8	25.43	3224.82	0.357	126.83	71.25	1.33	0.039	M	-0.081
9	27.56	3735.14	0.569	135.53	48.42	1.67	0.068	M	-0.824
10	23.43	2841.94	0.562	121.29	41.69	1.70	0.114	M	-0.996
11	17.93	400.99	1.207	22.35	14.86	1.22	0.020	G	0.925
12	81.52	13382.07	0.642	164.15	127.05	1.13	0.008	M	-0.866
13	16.72	8901.65	0.728	532.55	22.96	4.81	0.078	G	0.968
14	60.89	3284.59	1.374	53.94	44.33	1.1	0.00033	G	0.967
15	18.83	2096.55	0.383	111.32	49.17	1.50	0.061	M	0.773
16	6.84	1978.43	0.359	289.41	19.06	3.89	0.210	M	0.772
17	57.47	4375.88	1.302	76.14	44.15	1.31	0.061	G	-0.521
18	63.79	3914.08	1.812	61.36	35.21	1.32	0.001	G	0.976
19	82.99	16195.15	0.480	195.15	172.95	1.06	0.001	M	-0.893
20	67.99	18898.4	1.327	277.97	51.24	2.33	0.084	G	-0.629
21	82.99	16195.15	0.480	195.15	172.95	1.06	0.001	M	-0.893
22	57.33	19289.45	1.420	336.46	40.37	2.88	0.155	G	-0.735
23	38.56	20479.6	0.253	531.09	152.15	1.86	0.035	M	-0.995
24	24.04	25972.84	0.239	1080.40	100.40	3.28	0.016	M	-0.993
25	26.25	14934.14	0.630	568.98	41.66	3.69	0.013	M	-0.998
26	38.72	7140.57	0.409	184.41	94.67	1.39	0.026	M	-0.985
27	34.78	1812.87	3.102	52.13	11.21	2.15	0.295	G	-0.984
28	33.76	2376.25	3.846	70.38	8.78	2.83	0.339	G	-0.985
29	82.04	828191.8	0.583	10095.46	140.77	8.46	0.036	M	-0.992
30	10.00	28222.19	0.547	2822.78	18.29	12.42	0.116	M	-0.996
31	81.99	493323.1	1.188	6016.79	68.99	9.33	0.069	G	-0.928

VES NO.	H (m)	T (Ωm^2)	S (Seimens)	ρ_t (Ωm)	ρ_l (Ωm)	λ	ϕ_f	*Aquifer Protective capacity	Reflection Coeff.
32	32.42	2268.91	3.77	69.99	8.60	2.85	0.33	G	0.99
33	7.42	23485.93	1.066	3167.35	6.96	21.33	0.157	G	-0.997
34	13.57	259.17	1.326	19.09	10.23	1.36	0.086	G	0.707
35	77.81	11944.05	0.665	153.49	117.02	1.14	0.012	M	-0.922
36	6.33	30355.09	1.032	4798.46	6.13	27.97	0.022	G	-0.999
37	15.24	21037.12	0.074	1380.38	205.96	2.58	0.029	P	-0.998
38	68.81	18272.92	0.274	265.54	251.18	1.02	0.00004	M	-0.945
39	6.51	5813.076	0.226	893.49	28.73	5.57	0.116	M	-0.829
40	100.00	18228.17	0.581	182.28	172.04	1.03	0.00010	M	0.675
41	47.01	5161.17	0.723	109.79	65.02	1.3	0.002	G	0.972
42	25.41	7131.56	3.896	280.64	6.52	6.56	0.213	G	-0.683
43	37.19	7310.98	0.272	196.59	136.73	1.2	0.007	M	0.228
44	21.58	20843.83	0.856	965.70	25.23	6.18	0.139	G	0.977
45	34.45	2481.53	13.022	72.04	2.65	5.22	0.195	E	0.999
46	33.75	1920.41	1.228	56.90	27.49	1.44	0.018	G	0.992
47	30.45	8467.88	0.366	278.11	83.21	1.83	0.065	M	-0.996
48	16.27	4838.22	0.886	297.28	18.37	4.02	0.144	G	-0.998
49	66.27	7178.20	11.518	108.32	5.75	4.34	0.031	E	-0.717
50	99.97	19175.66	0.632	191.80	158.19	1.1	0.00027	M	-0.990
51	46.30	21392.38	0.296	462.04	156.29	1.72	0.004	M	-0.996
52	99.97	14726.93	0.830	147.31	120.50	1.1	0.002	G	-0.761
53	99.97	16942.92	0.867	169.47	115.26	1.21	0.022	G	-0.800
54	97.71	9295.81	1.346	95.13	72.57	1.14	0.00040	G	-0.762

*Aquifer Protective capacity: E- Excellent; G- Good; M- Moderate; W- Weak; P- Poor

The total resistance of the current flowing perpendicular to the layers will be the sum of resistance offered by each layer and can be expressed as follows,

$$T = \sum_{i=1}^{n} h_i * \rho_i \qquad (1)$$

This is the "transverse resistance".
The transverse resistivity to the current flowing perpendicular to the layers is given by,

$$\rho_t = T/H \qquad (2)$$

where $H = \sum h_i$
H is the depth to the bottom most geoelectric layer.

The longitudinal conductance of the current flowing parallel to the layers is given by,
n

$$S = \sum_{i=1} h_i / \rho_i \qquad (3)$$

The longitudinal resistivity of the current flowing parallel to the layers is given by,

$$\rho_l = H/S \qquad (4)$$

Flathe (1955) reported that the transverse resistivity (ρ_t) is always greater than the longitudinal resistivity (ρ_l), unless the medium is uniform, wherein both ρ_t and ρ_l will be equal. This dependence of the resistivity on the direction of the current flow is known as anisotropy (λ) and the coefficient of pseudo anisotropy (λ) is given by using equations (3) and (4) as,

$$\lambda = \sqrt{(\rho_t/\rho_l)} \qquad (5)$$

Fracture porosities linked with tectonic fracturing of rocks were estimated using the expression derived by Lane et al. (1995),

$$\varphi_f = 3.41*10^4 (N-1)(N^2-1)/N^2C(\rho_{max}-\rho_{min}) \qquad (6)$$

where φ_f is the fracture porosity; N is the vertical anisotropy, (for Schlumberger 1-D data, both coefficient of electrical anisotropy (λ) and N are equal); ρ_{max} and ρ_{min} is the maximum and minimum apparent resistivity (Ω-m) respectively; while C is the specific conductance of groundwater in μS/cm, which is averaged to 610 μS/cm from bore wells and dug wells of the study area. This is done in order to draw a correlation between electrical anisotropy and fracture porosity of the study area.

Fracture geometry plays an important role in the trap covered hard rock terrain for groundwater exploration. It is also observed that high values of electrical anisotropy (λ) signify diverse degrees of fracturing, with enhanced water-holding capacity in hard rock areas (Kumar et al., 2014). In order to understand the degree of fracturing in the underlying basement, several researchers estimated reflection coefficient (k) (Olayinka 1996; Olasehinde and Bayewu 2011; Bhattacharya and Shalivahan, 2016). Reflection coefficient is non-dimensional and it is the interface separating two layers of different resistivity (ρ_1, ρ_2) values underneath the surface of the earth. The value of k ranges between +1 to -1 for any value of ρ_1 and ρ_2. If $\rho_2<\rho_1$, the flow of current lines will propagate in downward direction since the lower resistivity below the interface results in an easier path for the current within the deeper zones. Hence the reflection coefficient will be negative. If the last layer is a pure insulator or pure conductor, then the k value will be + 1 or -1 respectively. It is further opined that lower values of reflection coefficient display weathered/fractured basement rock and hence has superior water retention capability (Olayinka, 1996). The reflection coefficient (k) was calculated as,

$$k = (\rho_n - \rho_{(n-1)})/ (\rho_n+\rho_{(n-1)}) \qquad (7)$$

where ρ_n is the layer resistivity of the n^{th} layer and $\rho_{(n-1)}$ is the layer resistivity overlying the n^{th} layer.

5. RESULTS AND DISCUSSIONS

In order to plot the spatial variation maps of geoelectric parameters, kriging interpolation scheme (via SURFER version 11) is used. For the clarity in discussion, the results obtained from Dar-Zarrouk parameters have been grouped in terms of the four sub-divisions viz. Shirpur, Sindkheda, Sakri and Dhule located in Dhule district. A total of 54 VES data has been analyzed to decipher the hydrogeological signatures of the aquifers (Fig. 2).

Longitudinal conductance (S):

The longitudinal conductance (S) plotted in Figure (3) varies from 0.074 to 3.89 Siemens with average value of 0.933 Siemens in the study area. In NE part of Shirpur sub-division, the S values at VES stations 27 to 34 vary from 0.54 S to 3.85 S. These high S values obtained are presumably due to the thick sequence of alluvium deposits of Tapi river basin. It is reported by Baride et al. (2017) that this region is covered by black cotton soil with calcified soil and clay having thickness ranging in excess of 4 m. Galin (1979) was of the view that the longitudinal conductance aids in differentiating the changes in the total thickness of the sub-surface low resistivity geo-materials.

Stations 15 to 26 cover the Sindkheda sub-division in the central part of the district. The longitudinal conductance here is varying from 0.239 S to 1.812 S (Fig. 3). The high S values were observed at VES 17, 18, 20 and 22 (1.302 S to 1.812 S). The region beneath VES 17 and 22 comprises of highly weathered basalts, while black cotton soil with clay is dominant below VES 18 and 20. The thickness of these soil type ranges from 4 to about 22 m, therefore giving rise to high conductance values.

The Sakri sub-division of the study area encompasses VES stations 1 to 14. From Figure (3), it is observed that all the stations show low S value, except VES 11 and 14 which has values of 1.2 S and 1.3 S respectively. This region comprises of hard compact basalts with weak fractures which is reflected as low conductance.

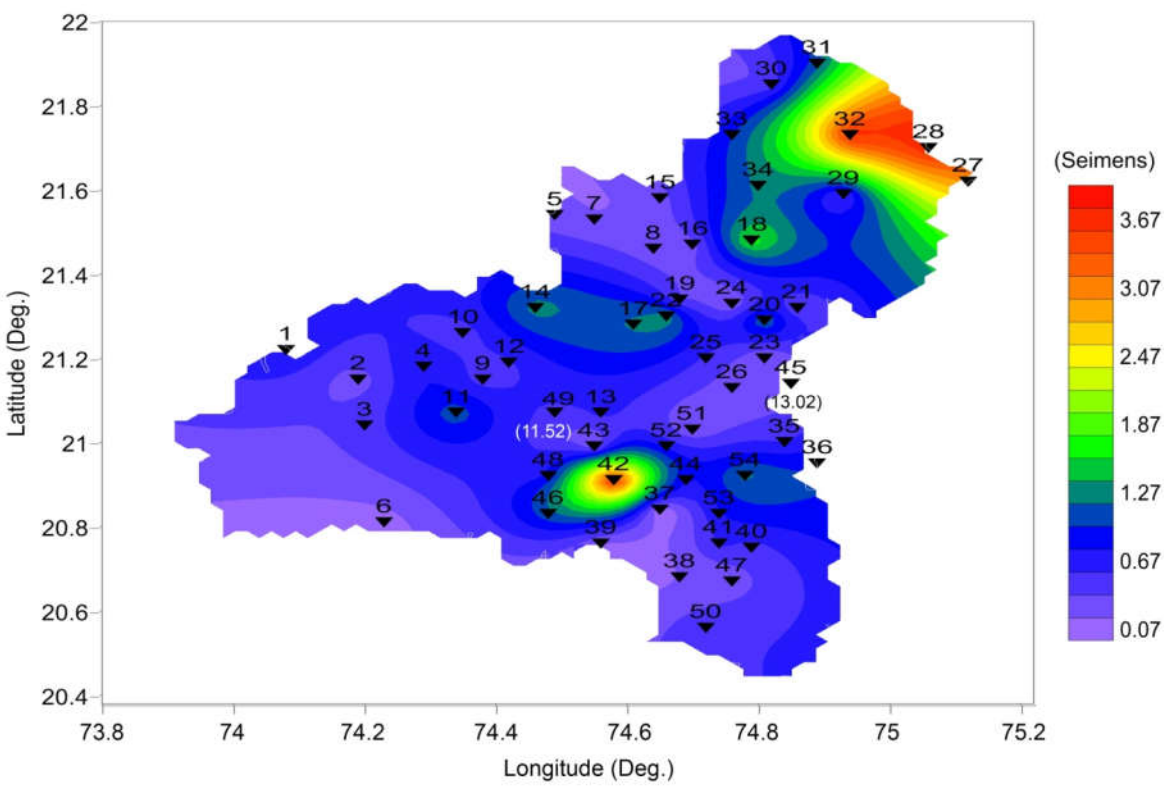

Figure 3: Spatial distribution of longitudinal conductance (S) in the study area.

A total of 20 VES stations occupy in Dhule subdivision (VES nos. 35-54). The longitudinal conductance varies from 0.074 S to 3.896 S with an average value of 0.84 S. Very low to low S values observed are due to the presence of hard and compact basalts, while high S values are due to weathered/fractured basalts. Very high *S* values were observed at VES 45 (13.02 S) and 49 (11.5 S) and were not considered during interpretation since it would mask the effects of other features in its vicinity. However, these values are marked on the Figure (3) and the *S* values are given in parenthesis.

It is reported that clayey overburden is characterized by high longitudinal conductance, which protects the underlying aquifer from contaminants (Oladapo et al., 2004). The earth acts as a natural filter to these contaminants from seeping through and its ability to check the infiltrating contaminants is a measure of its protective capacity. A modified classification of aquifer protective capacity rating is given by Oladapo et al. (2004), which facilitate to categorize an area into poor, weak, moderate, good, very good and excellent protective capacity zones (Table 2).

Table 2: Modified longitudinal conductance/protective capacity ratings (after Oladapo et al., 2004)

Longitudinal Conductance (Seimens)	**Protective Capacity rating**
> 10	Excellent
5-10	Very good
0.8-4.9	Good
0.2-0.79	Moderate
0.1-0.19	Weak
<0.1	Poor

The protective capacity of aquifers in the study area is estimated using S values reveals that about 44% area falls under the "good" aquifer protective capacity, while 48% is observed to have "moderate" aquifer protective capacity. A total of 2% each is characterized by "weak" and "poor" aquifer protective capacity and 4% depict "excellent" protective capacity ratings.

VES 6 situated in the south west part of Sakri sub-division is the only station to have weak protective capacity, characterized by low longitudinal conductance (0.169 S), which is also covered with weakly fractured and hard compact basalt. Similarly, VES 37 in Dhule sub-division is the only station offering poor protection to the underlying aquifers, which is possibly due to hard and compact basalt prevailing at this site. This station is also characterized by lowest longitudinal conductance (0.074 S) and relatively high transverse resistance (21037.1 Ωm^2) values. However, VES stations VES 45 (13.02 S) and 49 (11.5 S) in Dhule sub-division constitutes of excellent aquifer protective capacity rating, possibly due to Panjhara River flowing through this place. It has been reported that relatively thick geological succession and clayey overburden is usually characterized by reasonably high longitudinal conductance and thus offers protection to the underlying aquifer from contaminants (George et al., 2014). This implies that a thick clayey/silty overburden of Panjhara River is offering protection to the aquifers in this region.

It is pertinent to mention here that there are a number of rivers and streams in the study region, particularly in the northern and southern part and thus clayey/silty overburden is characterized by relatively high longitudinal conductance, offering protection to the underlying aquifers. Further from Figure (3), it can be surmised that the north eastern, central and southern parts of the study area divulge good to excellent protective capacity rating as can be seen from the high longitudinal conductance values. The low value of the protective capacity is a consequence of the absence of significant amount of clay as an overburden impermeable material (Obiora et al., 2015).

Transverse resistance (T):

The transverse resistance (T) contour map with a contour interval of 4000 Ωm^2 is shown in Figure (4). The T values in entire study area vary from a minimum of 259 Ωm^2 at VES 34 to a maximum of 37260 Ωm^2 at VES 5. High to moderately high transverse resistance is observed in NW, east and SE parts of the study area. Two stations (VES 29 and 31) were not considered for interpretation since it reflected very high T values of 493000 and 828000 Ωm^2 respectively.

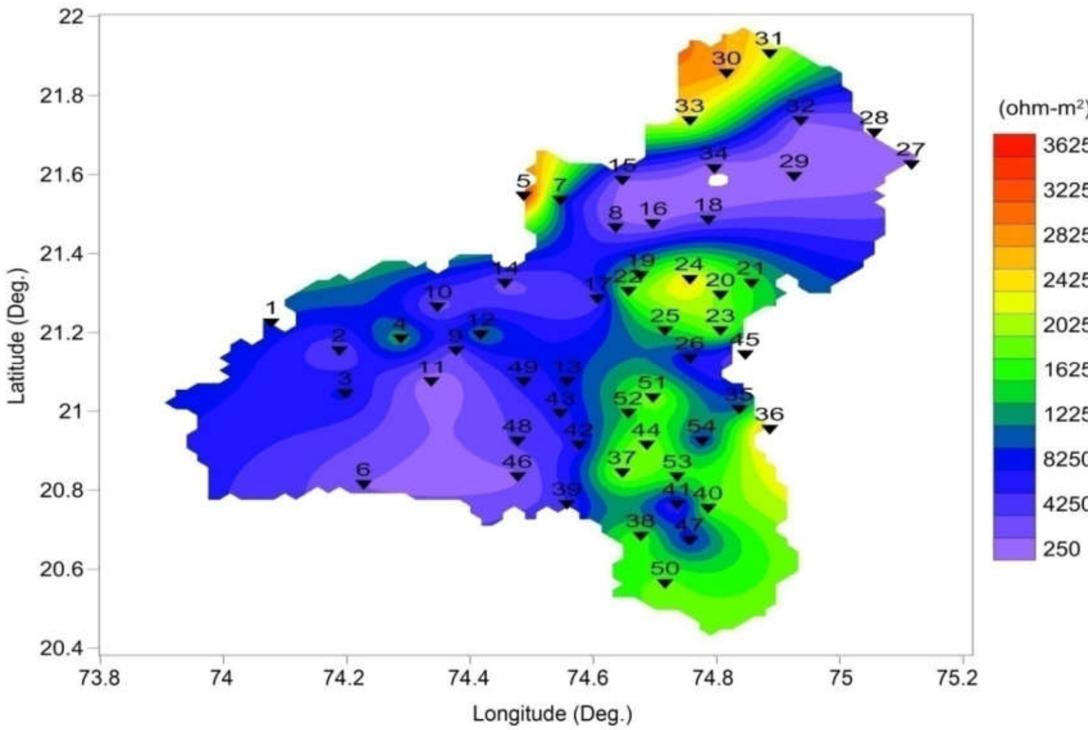

Figure 4: Spatial distribution of transverse resistance (T) in the study area.

In the north-western part, VES 5, 33 and 30 reveal high T values in the range of 23000 Ωm² to 37000 Ωm² (Fig. 4). It is reported by Baride et al. (2017) that this region comprises of thick layers of highly weathered and fractured basalt, black cotton soil with sand and occasional clays. Perhaps the thick layers of weathered and fractured basalts are responsible for the high values of T. This also indicates that the region is likely to have high transmissivity and thus more permeable to water movement and produce high yield of aquifers (Braga et al., 2006).

The eastern side of the study area consists of seven VES sites which show high T values (Fig. 4). Further, VES 24 is characterized by very high T values of the order of about 26000 Ωm², indicative of freshwater zone. Further southeast, the T value ranges from 12000 to about 30000 Ωm². The northeast and southwest parts of the study area are characterized by very low T values (<10000 Ωm²).

Parts of Sindkheda and Dhule sub-divisions (viz. surroundings of VES 24) is covered with weakly fractured and weathered basalts with a thin veener of black cotton soil/ murum in between (Baride et al. 2017) hence the T values there is ranging between 16000-20000 Ωm². Tahama et al. (2018) is of view that T values above 10000 Ωm² signify the fresh water aquifers in the Deccan Volcanic Province of Maharashtra.

Electrical Anisotropy (λ):

In most of the geological conditions, the coefficient of anisotropy (λ) is normally 1 and rarely exceeds 2 (Zohdy et al., 1974). However, Keller and Frischknecht (1966) are of the view that this value increases in hard and compact formation. In the present study area, electrical anisotropy (λ) values of 49 VES stations ranging from 1.028 (VES 38) to 6.55 (VES 42) with mean value of 2.198 is shown in Figure (5).

It is observed from Figure (5) that majority of the VES locations in Sakri, Sindkheda and Dhule sub-divisions portray λ value less than 2. About 16 locations with λ value greater than 2 are observed throughout the region. It can be observed from Figure (5) that the coefficient of anisotropy suggests an increasing trend from southwest to northeast direction with λ value >1.4. Another minor increasing trend is also seen in the northwest to southeast direction at the central part of the study area near VES 16. This suggests that the area is highly heterogeneous and fractures are dominant, thereby enhancing the prospects of groundwater.

As the study area is infested by numerous criss-crossing lineaments and dyke swarms, the lineaments in the study region are redrawn and superimposed on the electrical anisotropy map (Fig. 5) (http://bhuvan.nrsc.gov.in/state/MH) for a better perception of the subsurface characteristics. The spatial variation of electrical anisotropy (Fig. 5) reveals high λ values near Dhule, marked by lineaments extending in all directions, which might be the surface expression of the dykes present here. These have better water-holding capacity from different directions. The intersection points of these criss-crossing lineaments are perhaps potential locales of groundwater.

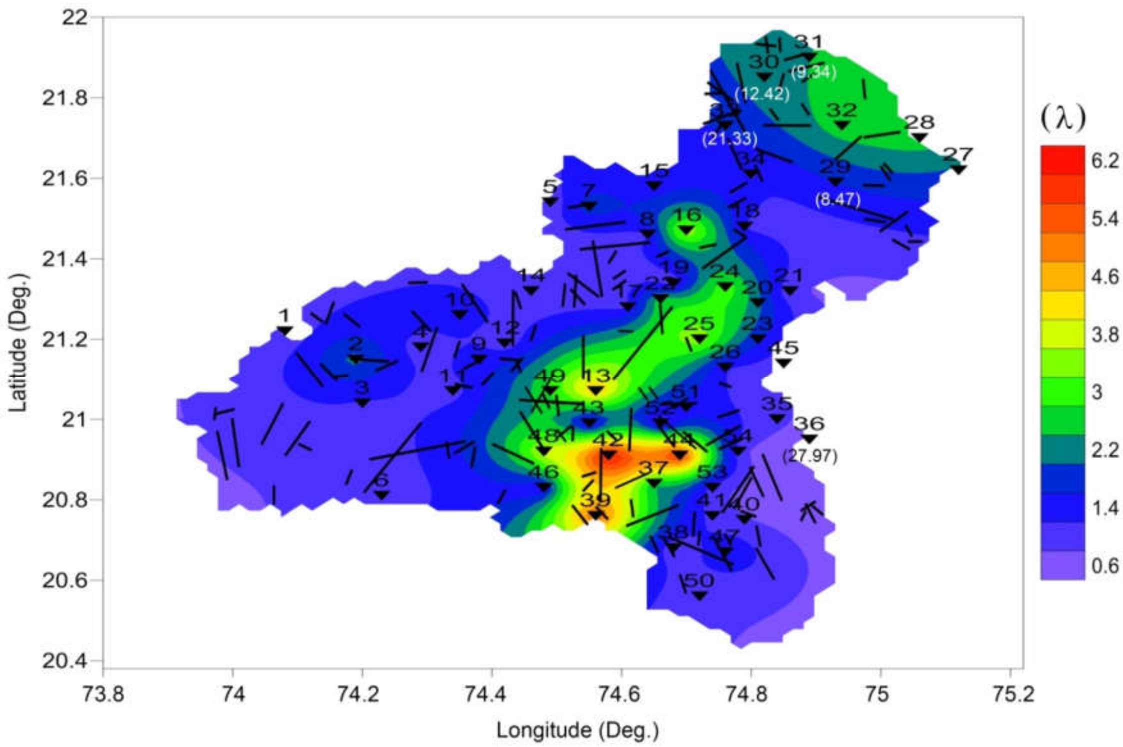

Figure 5: Spatial distribution of electrical anisotropy (λ) in the study area. The lineaments are also marked on the map.

Due to very high λ values (> 6), a total of 5 sounding points were not considered during interpretation of electrical anisotropy spatial variation, as it would mask the effects of other features in its vicinity. However, these are marked on the Figure (5) and the λ values are given in parenthesis. In the present case, it could be inferred that if λ exceeds 1, then the subsurface basaltic formation is more fractured; on the other hand, if the value of λ is about 1, then probably the overburden thickness is more (Kumar et al., 2014). In the present study, the maps of electrical anisotropy and aquifer zone thickness suggest that the VES stations with relatively thick overburden are hovering around the λ value of 1 (Fig. 6).

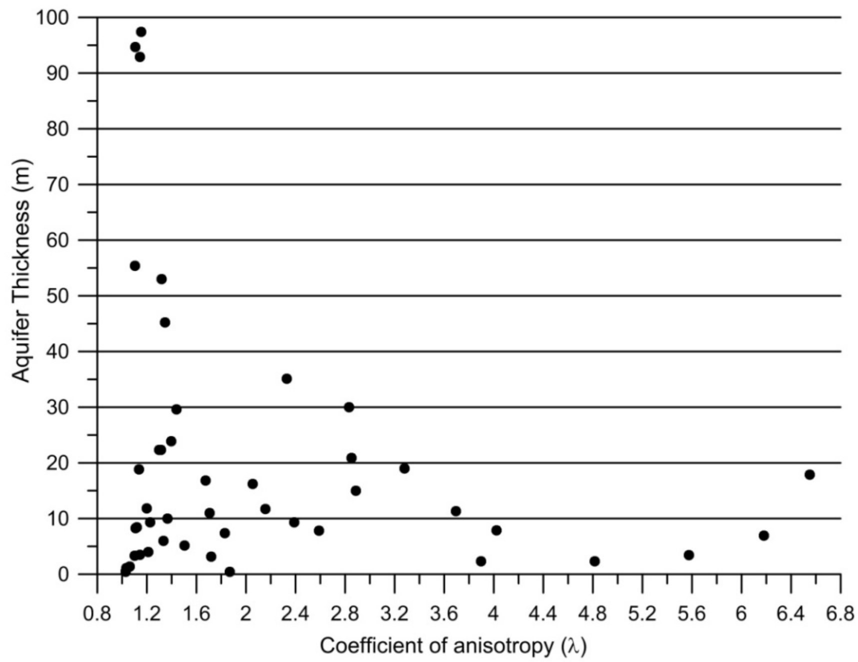

Figure 6: Plot of coefficient of anisotropy (λ) and aquifer zone thickness with VES numbers.

Fracture porosity (φ_f):

The fracture porosity (φ_f) values divulge higher porosities on the north, north-eastern and southern parts of the study area (Fig. 7). A maximum porosity value of 0.34 was observed in the north eastern part at VES 28, while VES 42 in the southern part revealed porosity values in the range 0.21. Minimum porosity value of 0.00004 was observed at VES 38 in the southern part.

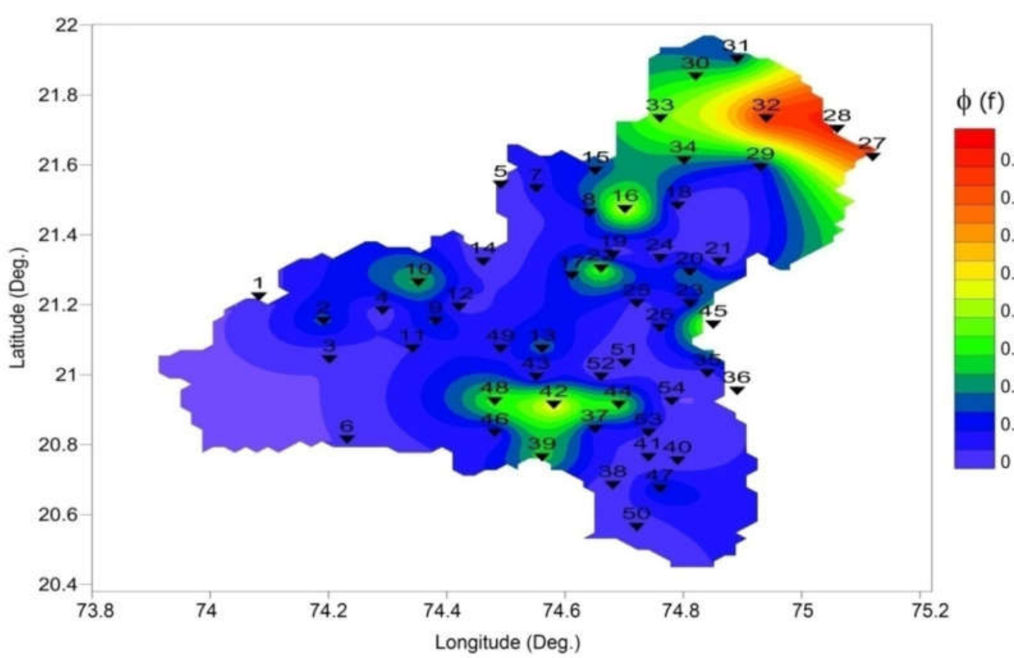

Figure 7: Spatial distribution of fracture porosity (φ_f) in the study area.

A look at the fracture porosity and anisotropy variations suggests that a positive correlation exists between these two parameters (Fig. 8). As mentioned earlier, the anisotropy values show an increasing trend in southwest to northeast directions, while another increasing trend is also observed from southeast to northwest direction. This suggests diverse degree of fracturing in multi direction, meaning that there is possibility that the fractured rocks are likely to possess water with better water withholding ability, ensuing in high porosity values (Niwas and Celik 2012).

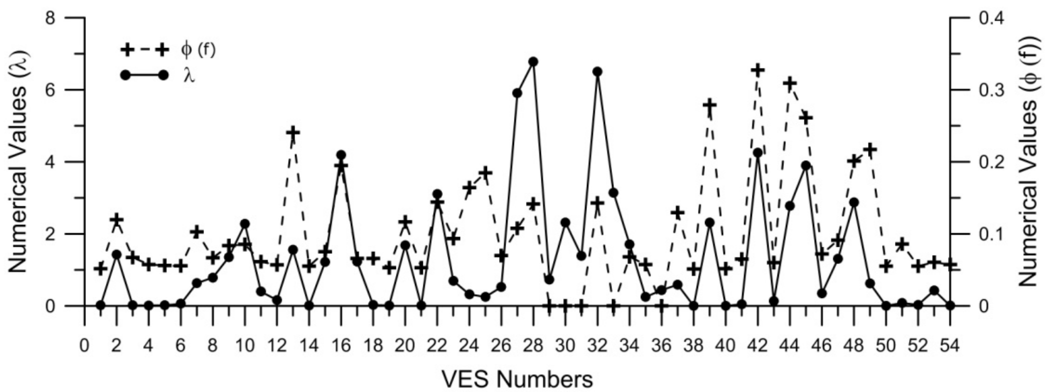

Figure 8: Plot of coefficient of anisotropy (λ) and fracture porosity (φ_f) with VES numbers.

Reflection coefficient (*k*):

The spatial variation of reflection coefficient (*k*) (Fig. 9) varies from +0.99 to -0.99, with an average of -0.34 in the study area. The negative average value of *k* indicates the dominancy of weathered and fractured zones having a low resistivity below a high resistivity groundwater repository. The Figure (10) shows that an inverse relation exists between reflection coefficient and anisotropy. It has been reported above that a positive correlation exists between anisotropy and fracture porosity. Hence, it can be understood that areas with low reflection coefficient signify both high electrical anisotropy and fracture porosity, suggesting weathered/ fractured rocks.

Based on topography, climate, rainfall and soil type, the Dhule district can be divided into Tapi valley and flat land regions (CGWB, 2013). The VES stations located in the north and north-eastern sectors which are also in the vicinity of Tapi basin, show low *k* values whereas the flat land and hilly (western and south-western) areas reveal high *k* values. It is also seen from Figure (9), that VES stations 37-39, 42, 47-48, 50, 53-54 in the south reflect negative k values. It is pertinent to mention here that Panjhara River and its tributary flows along these sounding sites. The spatial variation map Figure (9), suggest that northern, north-eastern and southern parts of the study area has low *k* values, indicative of high aquifer thickness (in the present case averaged to 15 m) as well as its prolificacy. Zone of low *k* reflects zone of fresh water repository as this implies a transition from effectively high porous aquifer to a semi-permeable aquifer. Also these aquifers reveal medium to good protective capacity, except VES 37 (showing poor aquifer capacity).

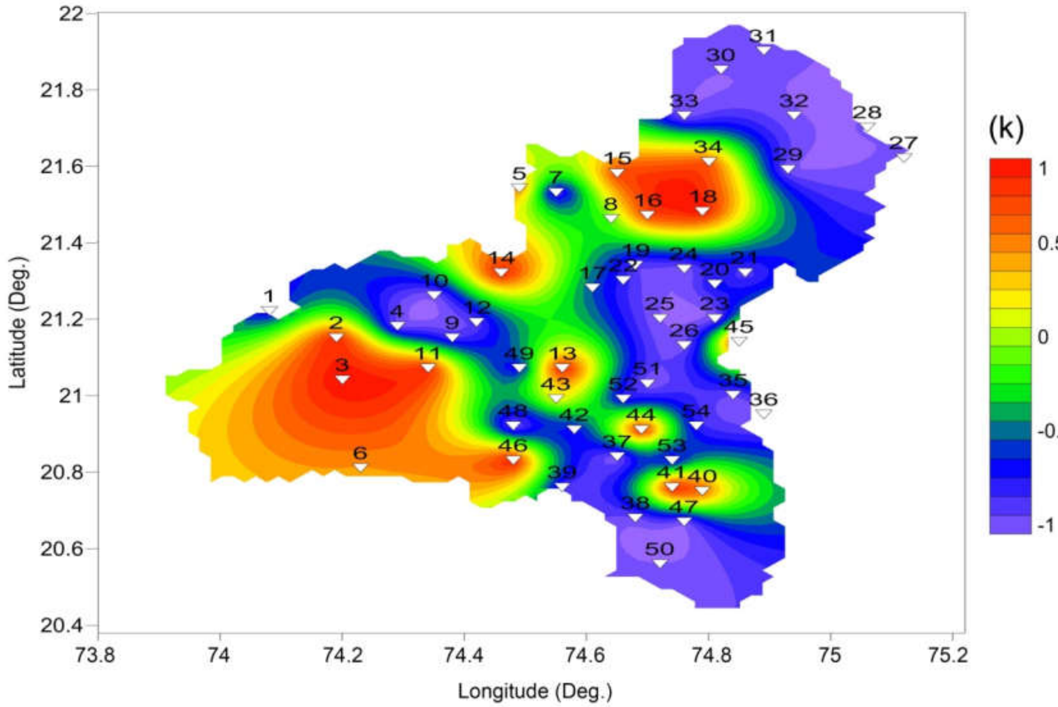

Figure 9: Spatial distribution of reflection coefficient (k) in the study area.

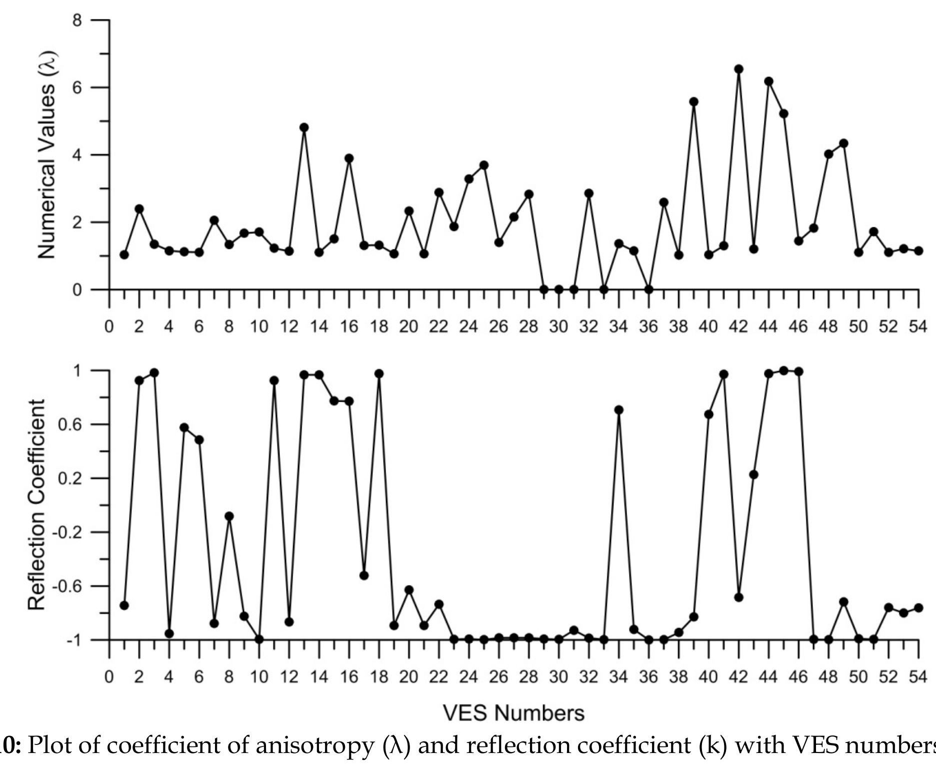

Figure 10: Plot of coefficient of anisotropy (λ) and reflection coefficient (k) with VES numbers.

6. CONCLUSIONS

To delineate aquiferous zones as well as the contribution from different geological features and formations providing protection to the aquifers, a total of 54 vertical electrical soundings (VES) have been carried out in the trap covered Dhule district, northern Maharashtra.

Analysis of secondary geophysical indices (Dar-Zarrouk and other associated parameters) is performed. The longitudinal conductance (S) value revealed a maximum of 13 to a minimum of 0.074 Siemens. High longitudinal conductance is evident in Shirpur, Dhule, Sindkheda in general and northern Sindkheda sub-division in particular. The high S values are manifestation of thick alluvium deposits, black cotton soil, calcified soil, occasional clays and highly weathered basalts. The protective capacity rating of the aquifers was deduced from the S values. About 92% of the study area is characterized by moderate to good protective capacity while 4% reveals excellent ratings. This implies that weathered/fractured rocks, thick soil and alluvial overburden are protecting the aquifers against infiltrating contaminants.

The total transverse resistance T varies from 259 to 37260 Ωm^2. High T values in excess of 12000 Ωm^2 are observed in parts of north-west, east and south-east of the study area signifying fresh water regime. This also reflects high transmissivity and, hence highly permeable to fluid movement.

The study area suggests heterogeneous nature of the subsurface as is revealed from the coefficient of electrical anisotropy (λ) with increasing trend in SW-NE and NW-SE directions, which are supposed to be more fractured. Several lineaments are criss-crossing the terrain and the intersection points of these are potential groundwater zones.

A positive relationship is observed between the electrical anisotropy and fracture porosity ensuring enhanced water withholding ability. On the other hand, low reflection coefficient values correspond to high λ values, signifying an inverse relationship between these two parameters. It is therefore advocated that these results will offer valuable and reliable information for a comprehensive groundwater development in hard-rock environs of the country.

ACKNOWLEDGEMENTS

The authors would like to thank the Director, IIG for providing the necessary facilities and permitting to publish this work. The authors express their gratitude to Dr. N.J. George, Physics Department, Akwa Ibom State University, Nigeria, for many fruitful discussions. Also, authors express their sincere thanks to Shri B.I. Panchal for drafting the figures with perfection.

REFERENCES

[1]. Baride, M.V., Patil, J.B., Baride A.M, Golekar, R.B. and Patil, S.N. (2017). Comparative study of Wenner and Schlumberger electrical resistivity method for groundwater investigation: a case study from Dhule district (M.S.), India. *Applied Water Science*. V. 7: 4321–4340, https://doi.org/10.1007/s13201-017-0576-7.

[2]. Beane, J.E., Turner, C.A., Hooper, P.R., Subbarao, K.V. and Walsh, J.N. (1986). Stratigraphy, composition and form of Deccan basalts, Western Ghats, India; *Bulletin of Volcanology*. V. 48: 61-83.

[3]. Bhattacharya, B.B. and Shalivahan (2016). *Geoelectric methods: Theory and application*; McGraw Hill Education (India). Pvt. Ltd, India.

[4]. http:// bhuvan.nrsc.gov.in/state/MH. Bhuvan: ISROs geoportal.

[5]. Bobachev, A. (2003). Resistivity Sounding Interpretation. IPI2WIN: Version 3.0.1 a 7.01.03. Moscow State University.

[6]. Braga, A.C.O., Filho, W.M. and Dourado, J.C. (2006). Resistivity (DC) method applied to aquifer protection studies. *Brazilian Journal of Geophysics*. 24(4): 573-581.

[7]. Central Ground Water Board (CGWB) (2013). Groundwater Information, Dhule district, Maharashtra. *Technical report No. 1799/DBR/2013*.

[8]. Dahlin, T. (2000). Electrode charge-up effects in DC resistivity data acquisition using multi electrode arrays. *Geophysical Prospecting*. V. 48(1)**:** 181-187.

[9]. Deolankar, S.B. (1980). The Deccan Basalt of Maharashtra, India- their potential as aquifers. *Ground Water*. V. 18(5): 434-437.

[10]. Deshmukh, S.S. and Sehgal, M.N. (1988). Mafic Dyke Swarms in Deccan Volcanic Province of M.P. and Maharashtra. *Memoir Geological Society of India*. V. 10: 323-340.

[11]. Duraiswami, R.A. (2005). Dykes as potential groundwater reservoirs in semi-arid areas of Sakri Taluka, District Dhule, of Maharashtra. *Gondwana Geological Magazine*. V. 20(1).

[12]. Erram, V.C., Gupta, G., Pawar, J.B., Kumar, S. and Pawar, N.J. (2010). Potential groundwater zones in parts of Dhule District, Maharashtra: a joint interpretation based on resistivity and magnetic data. *Journal of Indian Geological Congress*. 2(1): 37-45.

[13]. Flathe, H. (1955). Possibilities and limitations in applying geoelectrical methods to hydrogeological problems in the coastal area of northwest Germany. *Geophysical Prospecting*. V. 3: 95-110.

[14]. Galin, D.L. (1979). Use of longitudinal conductance in vertical electrical sounding induced potential method for solving hydrogeologic problems. Vestrik Moskovskogo University Geology. V. 34: 74-100.

[15]. Geological Survey of India (GSI) (2001). District resource map – Dhule district, Maharashtra. Geol. Surv. India.

[16]. George, N.J., Ekong, U.N. and Etuk S.E. (2014). Assessment of economically accessible groundwater reserve and its protective capacity in Eastern Obolo Local Government Area of Akwa Ibom State, Nigeria, using electrical resistivity method. International Journal of Geophysics. 1-10, 10.1155/2014/578981

[17]. Henriet, J.P. (1976). Direct application of Dar–Zarrouk parameters in ground water surveys. *Geophysical Prospecting*. 24: 344-353.

[18]. Keller, G.V. and Frischknecht, F.C. (1966). Electrical methods in geophysical prospecting. Oxford, Pergamon Press Inc.

[19]. Kumar, D., Rai, S.N., Thiagarajan, S. and Ratnakumari, Y. (2014). Evaluation of heterogeneous aquifers in hard rocks from resistivity sounding data in parts of Kalmeshwar taluk of Nagpur district, India. *Current Science*. V. 107(7): 1137-1145.

[20]. Lane, Jr. J.W., Haeni, F.P. and Watson, W.M. (1995). Use of a square array direct current resistivity method to detect fractures in crystalline bedrock in New Hampshire. *Ground Water*. V. 33(3): 476-485.

[21]. Maillet, R. (1947). The fundamental equation of electrical prospecting. *Geophysics*. V. 12: 529-556.

[22]. Nilsen, K.H., Sydnes, M., Gudmundsson, A. And Larsen, B.T. (2003). How dykes affect Groundwater transport in the northern part of the Oslo Graben. *Geophysical Research Abstracts*. V. 5: 09684.

[23]. Niwas, S. and Celik, M. (2012). Equation estimation of porosity and hydraulic conductivity of Ruhrtal aquifer in Germany using near surface geophysics. Journal of Applied Geophysics. V. 84: 77-85.

[24]. Obiora, D.N., Ajala, A.E. and Ibuot, J.C. (2015). Evaluation of aquifer protective capacity of overburden unit and soil corrosivity in Makurdi, Benue State, Nigeria, using electrical resistivity method. *Journal Earth System Science*. 124(1): 125-135.

[25]. Oladapo, M.I., Mohammed, M.Z., Adeoye, O.O. and Adetola, B.A. (2004). Geoelectrical investigation of the Ondo State Housing Corporation Estate, Ijapo Akure, Southwestern Nigeria. *Journal of Mining and Geology*. V. 40(1): 41-48.

[26]. Olasehinde, P.I. and Bayewu, O.O. (2011). Evaluation of electrical resistivity anisotropy in geological mapping: A case study of Odo Ara, West Central Nigeria. *African Journal of Environmental Science and Technology*. V. 5(7): 553-566.

[27]. Olayinka, A.I. (1996). Non Uniqueness in the Interpretation of Bedrock Resistivity from Sounding Curves and its Hydrological Implications. *Water Resources Journal of Nigerian Association of Hydrogeologists*. 7(1-2): 55-60.

[28]. Pawar, N.J. and Shaikh, I.J. (1995). Nitrate pollution of groundwaters from shallow basaltic aquifers. Deccan Trap hydrogeologic province, India. *Environmental Geology*. V. 25: 197-204.

[29]. Qureshy, M.N. (1981). Gravity anomalies, isostacy and crust mantle relations in the Deccan trap and contiguous regions in *Deccan Volcanism*, ed. Subba Rao, K.V. and Sukeshwala, R.N., *Geological Society of India Memoir*. No. 3: 184-197.

[30]. Rai, S.N., Thiagarajan, S., Ratnakumari, Y., Anand Rao, V. and Manglik, A. (2013). Delineation of aquifers in basaltic hard rock terrain using vertical electrical soundings data. *Journal of Earth System Science*. 122(1): 29-41.

[31]. Shailaja, G., Laxminarayana, M., Patil, J.D., Erram, V.C., Suryawanshi, R.A. and Gupta, G. (2016). Efficacy of anisotropic properties in groundwater exploration from geoelectric sounding over trap covered terrain. *Journal of Indian Geophysical Union*. 20(5): 453-461.

[32]. Sheth, H.C. (2005). Were the Deccan Flood Basalts derived in part from ancient oceanic crust within the Indian Continental lithosphere? Gondwana Research. V. 8(2): 109-127.

[33]. Singh, R.P. and Jamal, A. (2002). Dykes as Groundwater Loci in Parts of Nashik District, Maharashtra. *Journal Geological Society of India*. V. 59(2): 143-146.

[34]. Subbarao, K.V., Ramasubbareddy, N. and Prasad, C.V.R.K. (1988). Geochemistry and Palaeomagnetism of dykes from Mandaleshwar region, Deccan Basaltic Province. *Geological Society of India Memoir*. No. 10: 225-233.

[35]. Subbarao, K.V., Chandrashekharam, D., Navaneethakrishanan, P. and Hooper, P.R. (1994). Stratigraphy and structure of parts of the central Deccan Basalt Province: Eruptive models. In : *Volcanism* (ed) K V Subbarao. pp. 321-332, Wiley Eastern, New Delhi.

[36]. Tahama, K., Gupta, G. and Krishnamacharyulu, S.K.G. (2018). Estimation of secondary geophysical indicators to demarcate sea water intrusion in parts of Konkan coast, Maharashtra. *Journal of Applied Hydrology*. V. XXXI – No.1-4.

[37]. Wadia, D.N. (1975). Geology of India. publ: Tata McGraw Hill Publishers, New Delhi, India, p. 276.

[38]. Widdowson, M. and Mitchell, C. (1999). Large scale stratigraphical, structural and geomorphological constraints for earthquakes in the southern Deccan traps, India: The case for denudationally driven seismicity, *Deccan Volcanic Province*, Ed. Subbarao, K.V., *Geological Society of India Memoir*. No. 43(1): 425-452.

[39]. Zohdy, A.A.R., Eaton, G.P. and Mabey, D.R. (1974). Application of surface geophysics to ground-water investigation. Techniques of water-resources investigations series of the United States Geological Survey, 2nd ed.